

## Effects of tendon damage on static and dynamic behavior of CFTA girder

Thuy Dung Vu<sup>1a</sup>, Sang Yoon Lee<sup>2b</sup>, Sandeep Chaudhary<sup>3c</sup> and Dookie Kim<sup>\*1</sup>

<sup>1</sup> Department of Civil and Environmental Engineering, Kunsan National University, Jeonbuk, Republic of Korea

<sup>2</sup> Structural Engineering & Bridge Research Division, Korea Institute of Construction Technology, Gyeonggi-Do, Republic of Korea

<sup>3</sup> Department of Civil Engineering, Malaviya National Institute of Technology Jaipur, India

(Received June 27, 2011, Revised June 10, 2013, Accepted August 14, 2013)

**Abstract.** Experimental studies and finite element analyses have been carried out to establish the effect of tendon damage on the structural behavior of concrete filled tubular tied arch girder (CFTA girder). The damage of tendon is considered in different stages by varying the number of damaged cables in the tendon. Static and dynamic structural parameters are observed at each stage. The results obtained from the experiments and numerical studies have been compared to validate the studies. The tendons whose damage can significantly affect the stiffness of the CFTA girder are identified by performing the sensitivity analysis. The locations in the girder which are sensitive to the tendon damage are also identified.

**Keywords:** bridge design; composite structure; concrete filled tubular tied arch; CFTA girder; dynamic behavior; static behaviour

### 1. Introduction

The concrete filled steel tubular (CFST) structures have been increasingly used recently owing to good structural performances by their high load-bearing capacity and energy dissipation ability. Combination of steel and concrete systems has been conceived as an efficient system on the premises that each type of material (steel and concrete) offers its natural advantage when utilized together (Chaudhary *et al.* 2009). The steel tube provides reinforcement and confinement along the length, thus minimizing the use of traditional longitudinal and transverse reinforcement cages, and preventing spalling of the concrete, whereas the in-filled concrete prolongs local buckling of the tube (Gardner and Jacobson 1967).

Extensive research has been carried out to investigate the structural behavior of CFST, which consists of different types of cross-section: circular hollow section (CHS), square hollow section (SHS) and rectangular hollow section (RHS); with different types of elements: column, beam-column and beam. These studies considered concrete filled (CF) thin-walled steel box (Ge

\*Corresponding author, Associate Professor, E-mail: kim2kie@chol.com

<sup>a</sup> Researcher, E-mail: vtdung1986@gmail.com

<sup>b</sup> Senior Researcher, E-mail: sylee@kict.re.kr

<sup>c</sup> Associate Professor, E-mail: sandeep.nitjaipur@gmail.com

and Usami 1992, 1994, 1996), CF box-shaped steel columns (Susantha *et al.* 2001), confined CFST with additional confinement (Xiao *et al.* 2005, 2010), high-strength CFST (Lee 2007), recycled aggregate CF steel tube (Yang *et al.* 2009), CF double skin (SHS outer and CHS inner) steel tubular (Han *et al.* 2006, 2009). The steel hollow section acts as formwork during casting as well as reinforcement for the concrete (Ge and Usami 1992, 1996, Han 2000). The concrete in turn, eliminates or delays the local buckling of steel hollow sections, and significantly increases the stiffness, strength and durability of the section (Shams and Saadeghvaziri 1999, Sakino *et al.* 2004).

In this paper, a new type of CFST structure, concrete filled tubular tied arch girder (CFTA girder) (Fig. 1), is presented in order to provide an efficient and aesthetic type of superstructure by way of combining existing types of superstructure. CFTA girder is an effective combination of innovative features of the CFST, arch and pre-stressed (PS) structures. It has been shown by Trinh *et al.* (2008) that CFTA girder offers a very competitive solution to the conventional reinforced concrete with the prominent characteristics. PS tendons and an arch shape reduce the bending moment and induce the compressive force to make up for tensile stress (Trinh *et al.* 2008). The efficiency of arch effect in CFST structures (Morcoux *et al.* 2010) is in proportion to the rise ratio, span length to girder depth,  $L/d$  (Fig. 3(a)). Since the greater efficiency of the arch effect requires lower girder depth, which governs the bending stiffness, it can be expected that its effect of CFTA girder is apparently limited. The optimization between the correlation of the increase of arch effect (according to an increase of the rise ratio) and the reduction of section stiffness is therefore more important in the design of CFTA girder. To be more efficient, the girder should be fixed at the ends, however, the ends of CFTA girder are not fixed (KICT 2010). PS tendons are therefore applied in order to maintain the arch shape as well as to sustain the external load. These tendons are located in the lower part and anchored at the ends of CFTA girder to compensate self weight loads and live loads effectively.

The design variables of CFTA girder include the rise ratio between the section depth at supports ( $d_1$ ) and at the middle ( $d_2$ ), the thickness of steel plate ( $t_s$ ), the PS tendon area ( $A_{PS}$ ) (Fig. 3(a)) and the concrete strength of arch block and slab. The first parameter is related to the aesthetic of CFTA girder. A survey of the correlation between the rise ratio and its aesthetic effect has been conducted by KICT (2010) and it has been revealed that the adequate value for the rise ratio is 0.4. The most critical factor in design of CFTA girder is the deformation due to live load. Based on a



Fig. 1 CFTA girder bridge

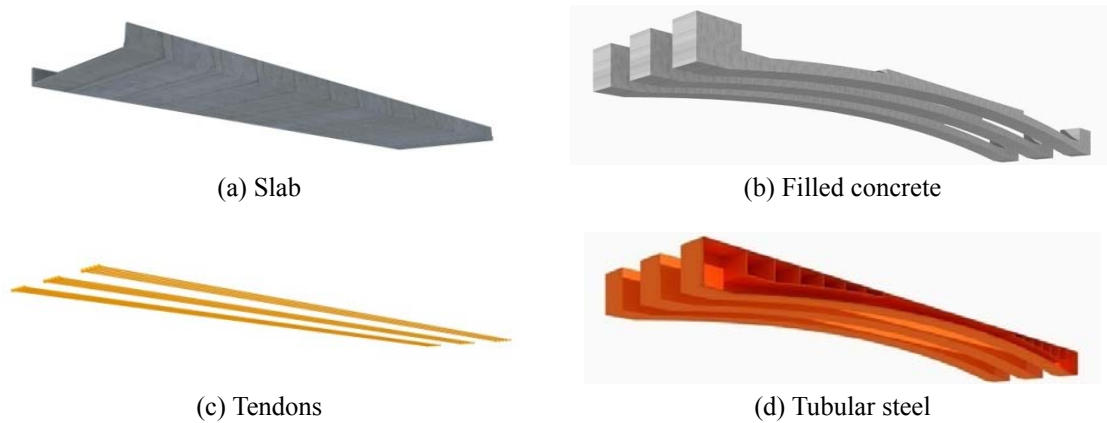


Fig. 2 Components of CFTA girder bridge

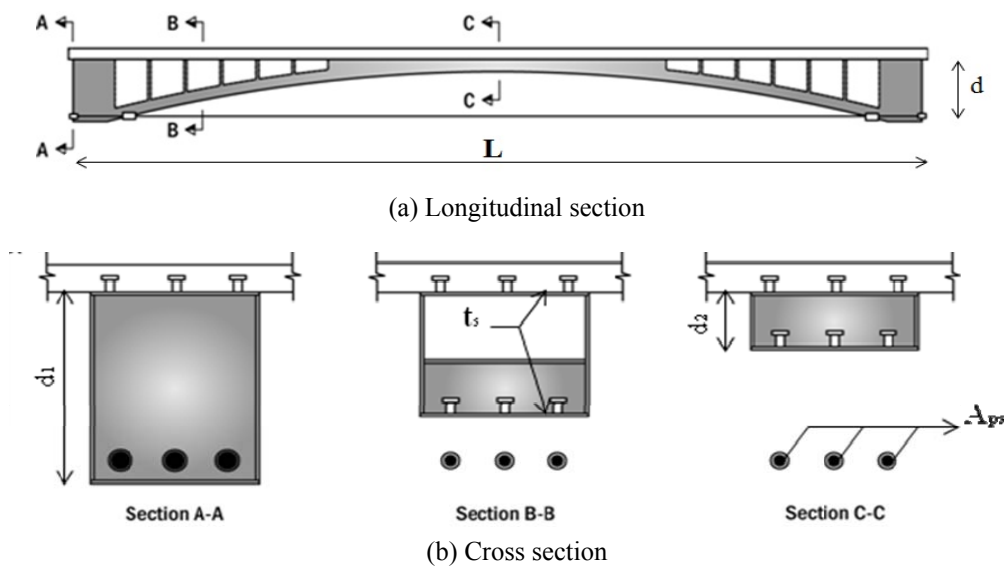


Fig. 3 Concept diagram of CFTA

sensitivity analysis (KICT 2010), under live load, the PS tendon is found to be largely affecting the deformation of CFTA girder while the steel plate thickness and the concrete strength are found to have small effect. It can therefore be concluded that the section depth at the supports and the PS tendon area are the key parameters in the performance of the CFTA girder. The former is decided by considering the construction site condition such as the longitudinal elevation and the overhead clearance. The later is decided according to the limit of deformation for given steel plate thickness (KICT 2010). Then, the allowable stress of concrete and steel can be satisfied by controlling the PS force. Fig. 4 presents the design flow chart of CFTA girder, including these considerations aforementioned.

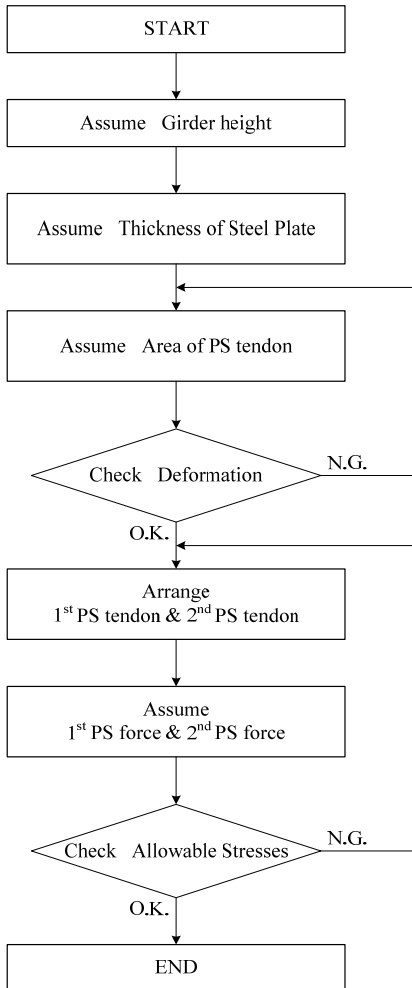


Fig. 4 CFTA design flow chart (KICT 2010)

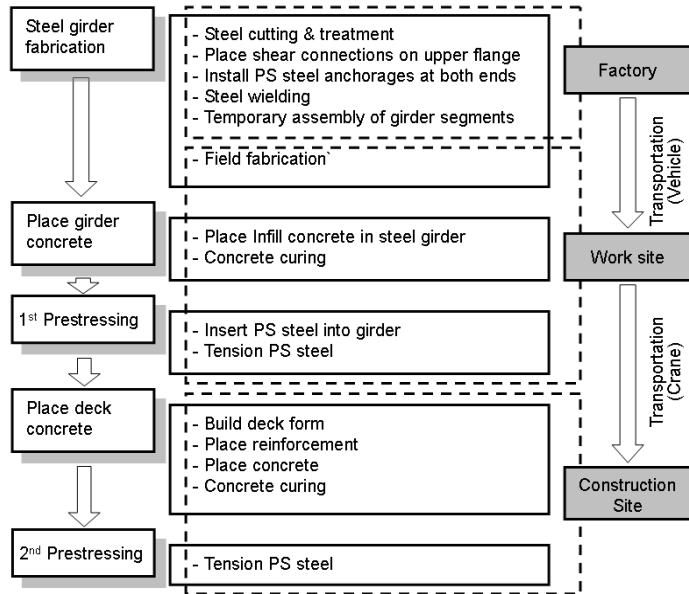


Fig. 5 CFTA construction procedure

The CFTA girder considered for this study comprises of four main components: tubular steel frame, concrete arch, tendon and concrete slab (Fig. 2). The shape and concept of CFTA girder are shown in Fig. 3. The arch shape is constructed by concrete blocks in order to transfer the self-weight load to the arch rib. These blocks are filled by pumping concrete into the tubular steel frame. The steel frame protects the concrete blocks as well as forms the shape of CFTA girder. Inside each block, there is a hollow space holding the concrete creating a very efficient composite section. Pre-stressing force is applied on tendons in two construction stages (Fig. 5): two inner PS tendons are tensioned in the first stage after constructing the arch girder and the two outer ones are tensioned in the next stage after pouring concrete of the slab. The second pre-stressing force is active after the girder is mounted on the abutment. As members of the structure, these four PS tendons have an influence on the behavior of CFTA girder. As the unbonded PS tendons, they resist only the tensile forces and cannot sustain a lateral load; their stabilities and working capacity

may be lost when damaged. The overall structure behavior then can be partly or entirely affected due to this tendon damage.

Therefore, the static and dynamic behavior of CFTA girder with a damaged tendon needs to be studied. The experimental tests have been carried out and a FE model using ABAQUS software has been developed in the present study for establishing the effect of tendon damage on the static and the dynamic behavior of CFTA girder. The results obtained from the experiments and numerical studies have been compared. The effect of tendon damage on the stiffness and concrete stress of CFTA girder is established by performing a sensitivity analysis.

## 2. Experimental setup of CFTA girder

A single span bridge of 30.6 m length has been constructed at Korea Institute of Construction Technology (KICT), South Korea. The specimen has been designed for the actual highway loading. Details of a typical cross-section, at the mid-span of the specimen, along with the details of PS tendon description are given in Table 1. The whole construction process except the fabrication of steel structure has been carried out in the laboratory. Specimen has been erected by a construction procedure shown in Fig. 5. Segments of the steel structure have been fabricated in the factory and then transferred to the laboratory. The strains and displacements have been measured to examine CFTA girder behavior in each construction stage. The strain gauge locations are illustrated in Fig. 6 in which SB is the bottom surface, ST is the top surface of the middle span cross section; and PS is the tendon. Fig. 7 shows the sensor layout installed at the lower surface of the girder. Measurements have been carried out on the specimen not only during the construction stages but also during the experimental load test.

Damage test on the specimen was performed by removing the outmost tendon, which consists of twelve small cables. The procedure of removing the tendon was conducted in three stages: three cables in the tendon were removed in the first stage; three more cables were removed in the next stage; and in the third stage, all cables were removed. The static and dynamic tests were performed after removing the cables in all three stages. Then, the tendon was again repaired and static and dynamic tests were again performed.

Table 1 Dimension of specimen and PS tendon

	Width	2.0 m	
Girder	Depth	End of span	1.75 m
		Middle of span	0.58 m
Slab	Effective width	3.5 m	
	Thickness	0.24 m	
Steel Plate	Thickness at the middle of span	Top flange	18 mm
		Bottom flange	18 mm
		Web	10 mm
PS Tendon	Inners	SWPC 7B $\Phi$ 15.2 mm 19 strands $\times$ 2 ducts	
	Outers	SWPC 7B $\Phi$ 15.2 mm 12 stands $\times$ 2 ducts	

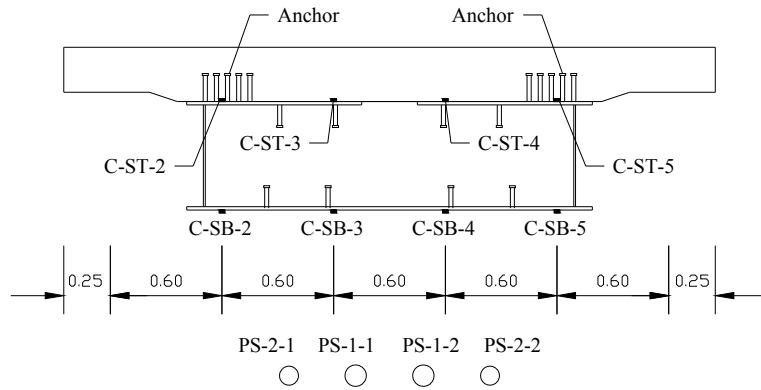


Fig. 6 Mid-span cross section (mm) and strain gauge locations for CFTA

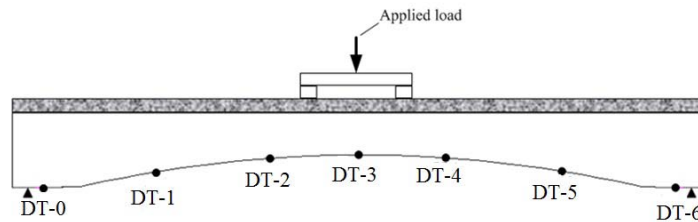


Fig. 7 Displacement sensor layout for static test

Static load test using a real-scale specimen has been carried out in order to verify the validity of CFTA finite element (FE) model presented in next section. The load has been applied by using two actuators having 350 kN loading capacity as illustrated in Figs. 8 and 9. Seven displacement sensors (Fig. 7) were evenly placed along one side, on the lower surface of CFTA girder, in order to measure the deformation. In the dynamic test, free vibrations were induced by using an exciter placed at two symmetric locations on CFTA slab (Fig. 10). The accelerometers were installed on the top surface of the slab along at the center line as shown in Fig. 11.

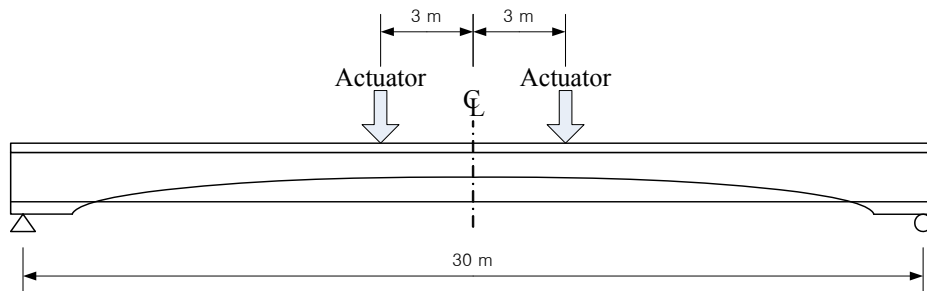


Fig. 8 Side view of experimental setting



Fig. 9 Overview of static test setup

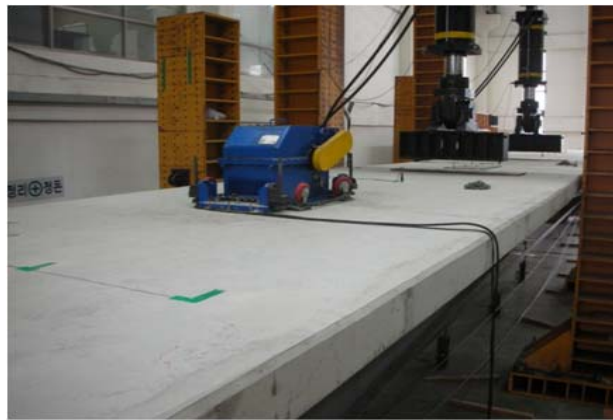


Fig. 10 Overview of dynamic test setup

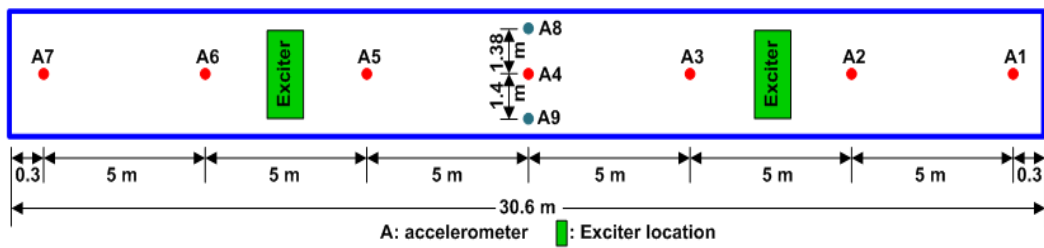


Fig. 11 Accelerometer sensor layout on slab top surface

### 3. Finite element model of CFTA girder

A finite element model has been developed using ABAQUS software for the CFTA girder considered in the experiment. This model comprises of four main components: tubular steel frame, concrete arch, PS tendon and concrete slab (Fig. 2). The steel frame is modeled as shell element and homogeneous steel section with 10 mm, 12 mm, and 22 mm of thickness. The pre-stressing forces for two inside and two outside tendons are taken as 844.57 MPa and 441.16 MPa, respectively. The slab is modeled as solid elements and the reinforcing bars were embedded as the two-node linear 3-D truss elements. The analysis takes into account the construction steps. The net displacements obtained for the FE model, at the end of the two tensioning stages and slab casting stage, are 37.9 mm, 23.9 mm and 65.0 mm, respectively. The full numerical simulation of CFTA girder is shown in Fig. 12.

The nonlinear mechanical properties of steel and tendon used in the simulation are presented in Table 2 (KICT 2010). Taking account of the strain rate-dependent plastic behavior of the structural steel, the isotropic strain hardening is considered. For slab and arch blocks, a conventional type of concrete (Knowles and Park 1969) with properties shown in Table 3 is considered. The equivalent load has been applied to cause approximately the same bending moment and axial force, at the middle of CFTA girder, as a design truck load effect in the experiment. The poisson's ratios are

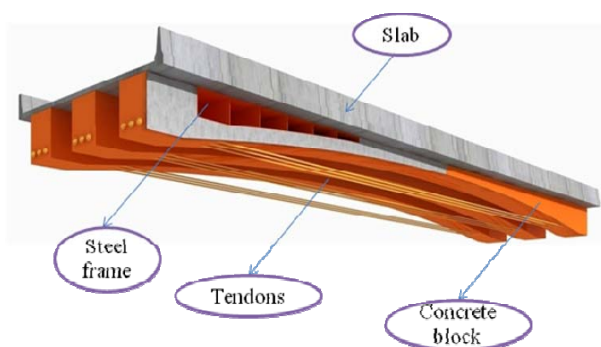


Fig. 12 Numerical model of CFTA

Table 2 Nonlinear properties of steel and tendon

Material	Yield stress (MPa)	Plastic strain
Steel	392.4	0.000
	392.4	0.018
	539.6	0.167
Tendons	1700.0	0.000
	1920.0	0.002
	2050.0	0.010
	2100.0	0.019
	2150.0	0.039

Table 3 Nonlinear properties of concrete

Compressive behavior			
Concrete on slab		Concrete on arch block	
Yield stress (MPa)	Inelastic strain	Yield stress (MPa)	Inelastic strain
15.3404	0.00000	22.585	0.0000
26.4416	0.00022	38.0605	0.00016
29.562	0.00045	43.1281	0.00034
30.6807	0.00076	45.1701	0.00006
29.8659	0.00109	44.2443	0.00009
27.2497	0.0015	40.9871	0.00124
15.3404	0.00262	22.585	0.00237
2.2704	0.00521	2.13423	0.00514
0.4023	0.01029	0.34981	0.01021

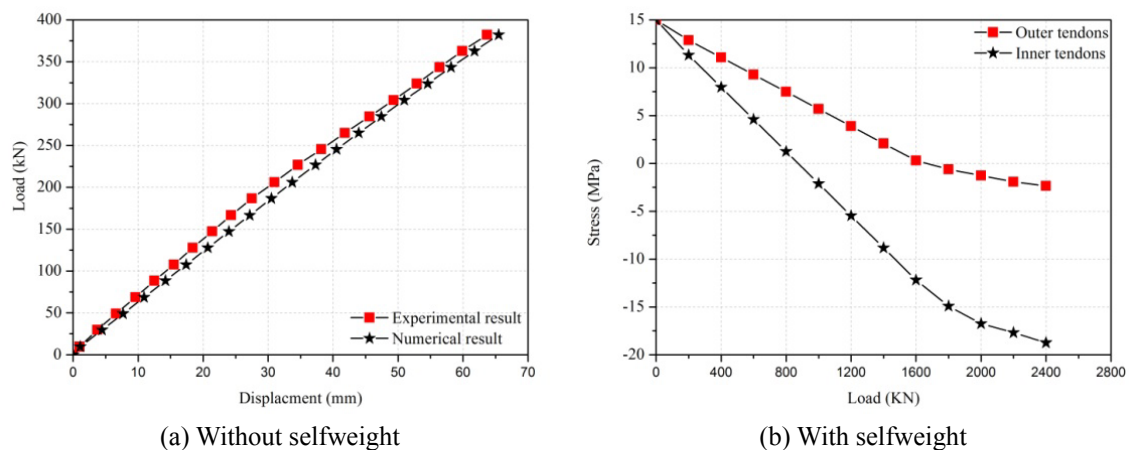


Fig. 13 Effects of PS tendons on concrete stress in CFTA

taken as 0.167 for steel and tendon and 0.3 for concrete. The density values for the steel, tendon and concrete are taken as  $78.5 \text{ kN/m}^3$ ,  $80 \text{ kN/m}^3$  and  $25 \text{ kN/m}^3$ , respectively.

#### 4. Sensitivity analysis

Sensitivity analysis is carried out to identify the effect of tendons on concrete stress and structure stiffness. Fig. 13 shows the effect of pre-stressing force in tendons on the concrete stress without self-weight load. It indicates that although all the four tendons affect CFTA behavior (as external load), the two inside tendons play a more important role in comparison with the two outside ones (Fig. 13(a)). A study on working of tendons against the self-weight load is also carried out by increasing pre-stressing force in steps (Fig. 13(b)). It shows that the stress in concrete block decreases rapidly with an increase in pre-stressing force.

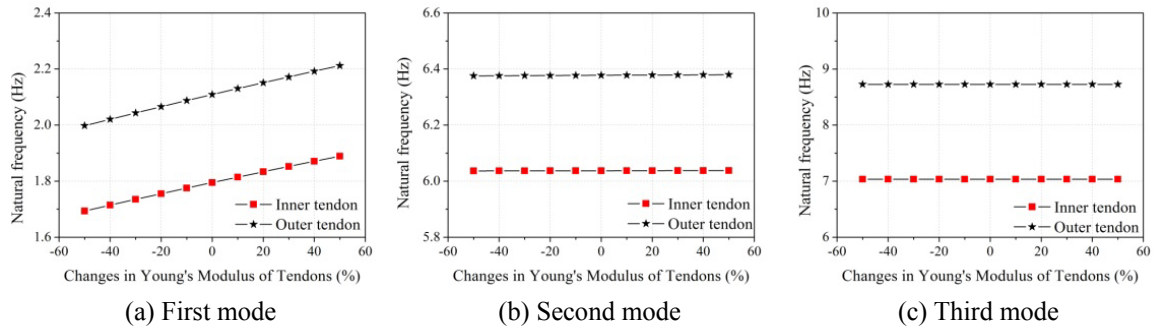


Fig. 14 Effects of tendons on CFTA stiffness

Table 4 Influence of tendons on natural frequency

Nature of modes	Natural frequencies (Hz)				
	Full	With 3 tendons	With 2 tendons	With 1 tendons	Without tendons
1 <sup>st</sup> Mode	2.1091	2.06696	1.99759	1.92473	1.87665
2 <sup>nd</sup> Mode	8.7265	8.72642	8.72636	8.7263	8.72626
3 <sup>rd</sup> Mode	19.716	19.7036	19.6828	19.6615	19.6477
4 <sup>th</sup> Mode	26.549	26.5273	26.4932	26.4589	26.4372
5 <sup>th</sup> Mode	36.737	36.7359	36.7358	36.7356	36.7349

The Young's modulus of tendon is varied to study the influence of tendon stiffness on CFTA behaviour. The value of Young's modulus was increased/ decreased by 10% in each step in order to identify its effect on the natural frequency. It is observed from the results shown in Fig. 14 that the changes in frequencies are found to be negligible. Numerical analysis was carried out using FE model with three tendons, two tendons, and one tendon as well no tendon. The natural frequencies obtained from this numerical analysis are shown in Table 4. It is observed that the tendons marginally increase the global stiffness (K) of CFTA girder.

## 5. Results and discussion

The results obtained from monitoring system at typical locations, ST and SB (Fig. 6), at each designed construction stage are shown in Figs. 15 and 16, respectively. The structural behavior of the CFTA specimen obtained by the FE model and the experiments is compared for each construction stage. The flexural deformations obtained by the numerical model and experiments are shown in Fig. 17. A close agreement is observed at different stages. It verifies the assumptions about deformation considered in the FE model. Fig. 18 shows the strain distribution curves along the depth during construction. Despite the larger compressive strain or the less loss in pre-stressing force of the specimen in 1<sup>st</sup> tensioning stage, the neutral axis existed at the similar depth. All these results indicate that the FEM model predict the behavior of CFTA girder very well.

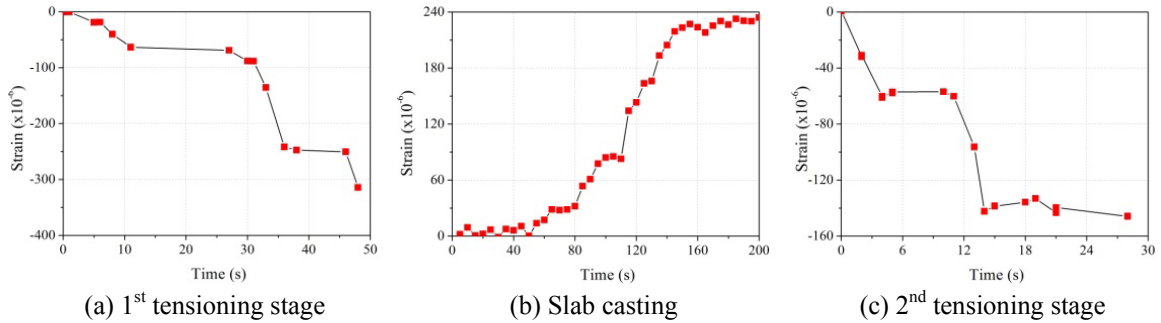


Fig. 15 Monitoring strain measured at SB location

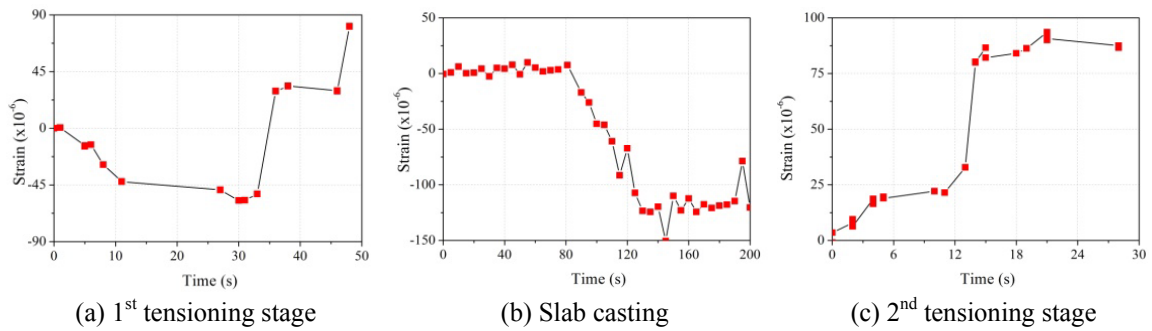


Fig. 16 Monitoring strain measured at ST location

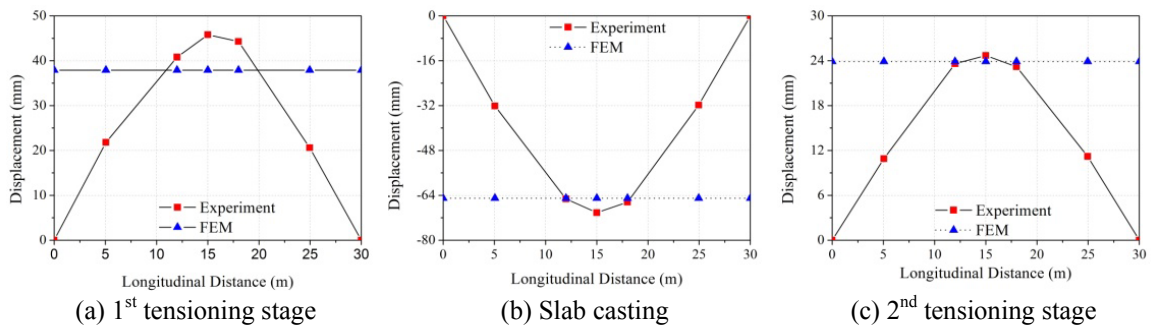


Fig. 17 Displacements obtained from experiment and FEM

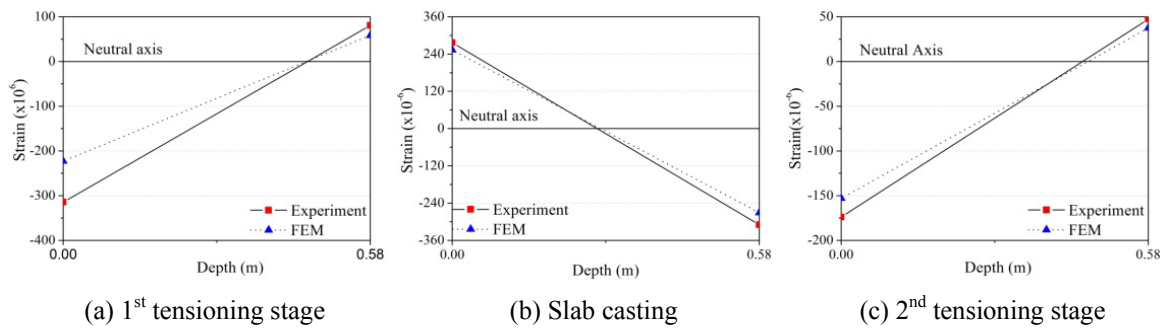


Fig. 18 Strains along the section depth

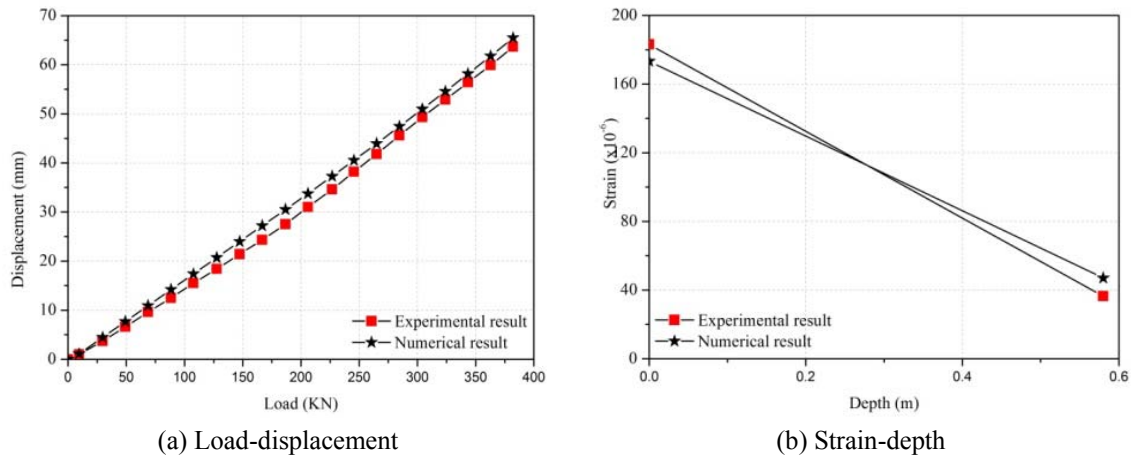


Fig. 19 Numerical and experimental behaviour under the design load

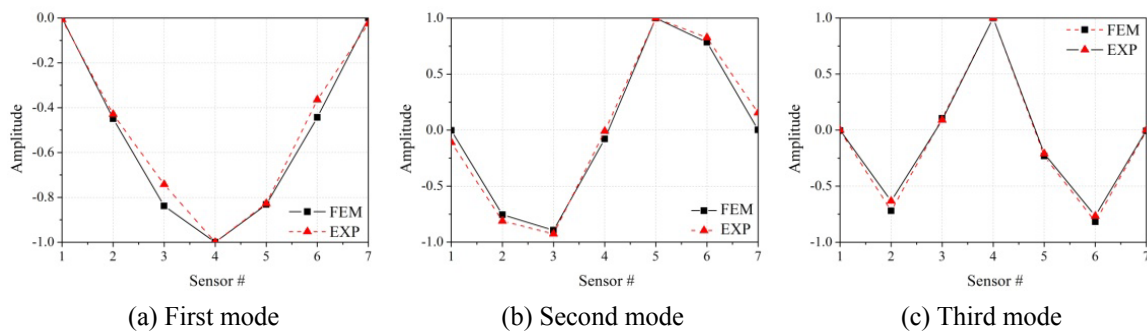


Fig. 20 Comparison of mode shapes obtained from the experiment and the FEM

Table 5 Comparison between numerical and experimental natural frequency

Nature of modes	Natural Frequencies (Hz)	
	FE model	Experiment
1 <sup>st</sup> Mode	2.1091	2.1973
2 <sup>nd</sup> Mode	8.7265	8.2031
3 <sup>rd</sup> Mode	17.716	16.4063

A comparison of the load-deformation curve as well as the strain-depth curve obtained from experiment and the numerical model under design load is shown in Fig. 19. Fig. 20 and Table 5 show a comparison of dynamic response in terms of mode-shape and natural frequency, respectively. A very good agreement is seen in the results of the FE model developed in this study and the experiments. It confirms that the FE model successfully predicts the static and dynamic behavior of CFTA girder. Accordingly, the effect of tendons on CFTA behavior can be well simulated by the numerical analysis.

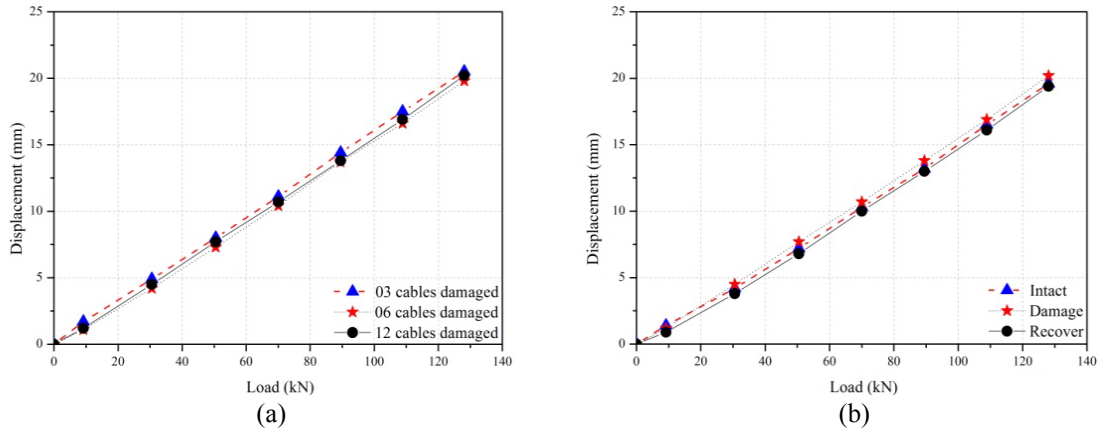


Fig. 21 Effect of tendon damage on displacement

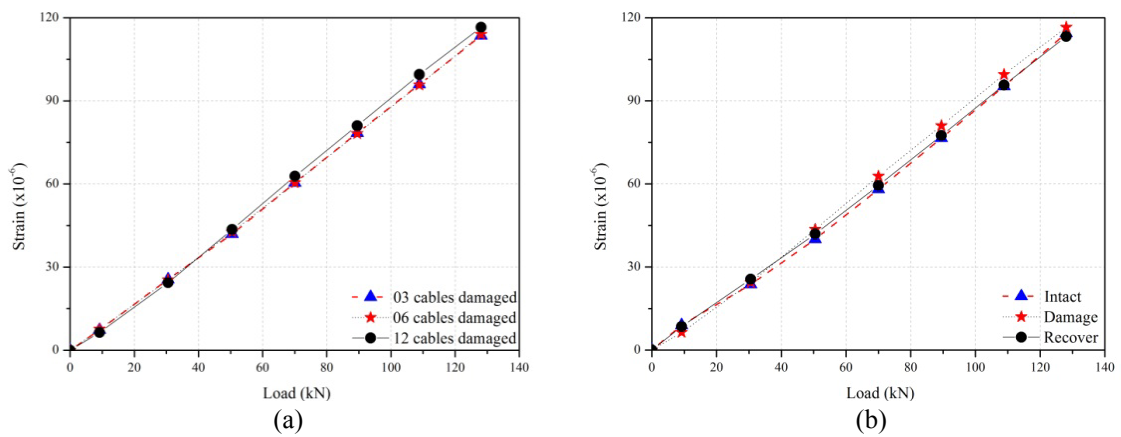


Fig. 22 Effect of tendon damage on strain at SB location

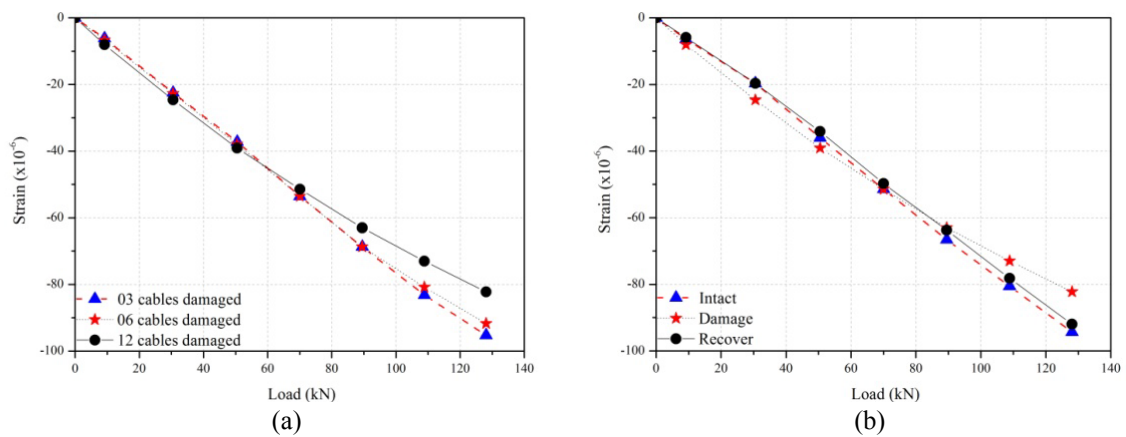


Fig. 23 Effect of tendon damage on strain at ST location

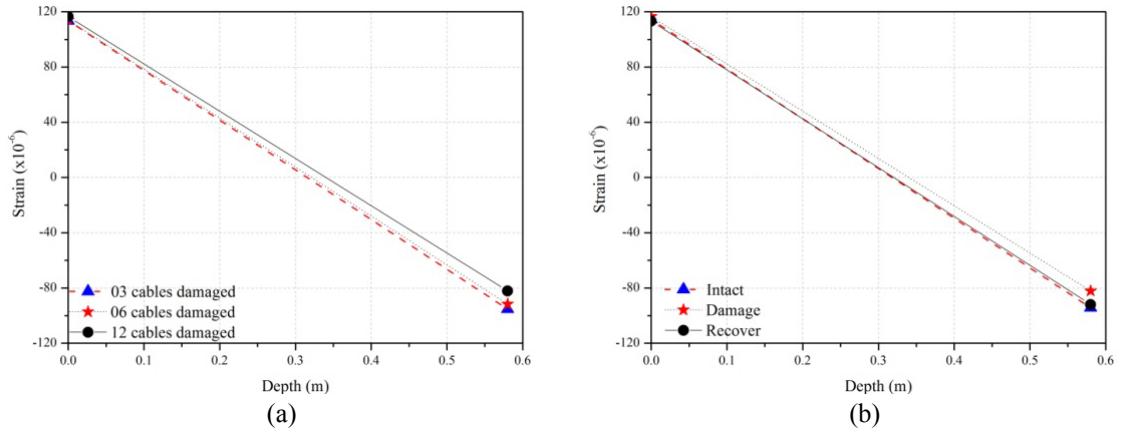


Fig. 24 Effect of the tendon damage on strain along section depth

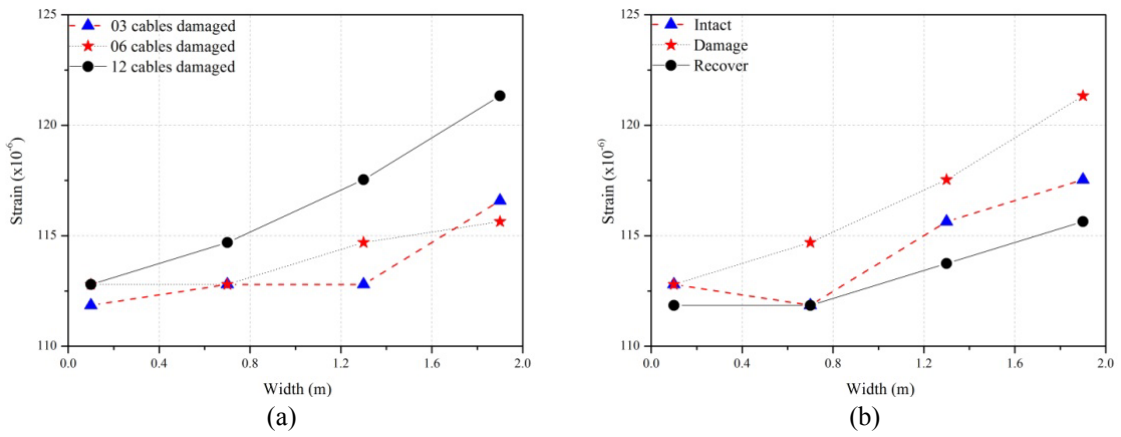


Fig. 25 Effect of tendon damage on strain along section width at SB location

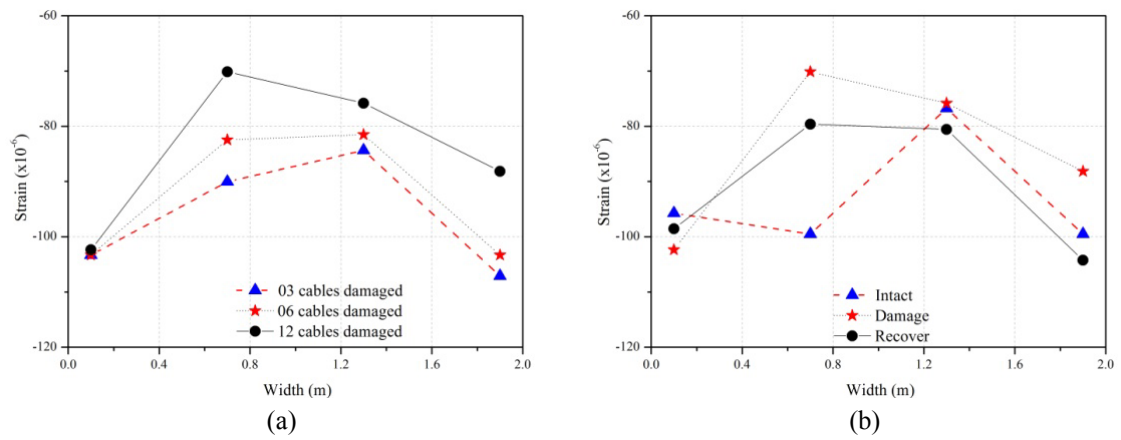


Fig. 26 Effect of tendon damage on strain along section width at ST location

The changes in strain along the depth and width at cross section C (Fig. 6) under the load of 128 kN are shown in Figs. 24-26. The variation of strain with depth (Fig. 24) reveals that the effect of damage at SB location, compressive surface, is more in comparison with that at ST location, tensile surface. Figs. 25 and 26 show that the most sensitive locations under damage are where anchors were installed for the bond between the arch block and the slab (the locations are shown in Fig. 6). It may be noted that the location C-ST 5 is more critical when damaged than the location C-ST 2.

The effect of the tendon on the concrete block stress and the global stiffness observed in Figs. 13 (b) and 14 increased the interest in the effect of tendon on the displacement as well as mode-shape and natural frequency of CFTA. The displacement under self weight force was therefore measured and compared between all three experimental damage cases considering loss of three cables, six cables and all of the cables as well as repaired tendon. The results are shown in Fig. 27. The large effect on displacement observed in the Fig. shows the important role of tendon, in the controlling the deformation of CFTA girder. The mode-shapes of the girder at the different damage stages are shown in Fig. 28 for mode-shape. The natural frequencies of the girder at the different damage stages are given in Table 6. It is observed that the mode-shape and natural frequency are not affected much by damage of the tendons. It reveals that CFTA dynamic characteristics are maintained in case of damage which may occur later.

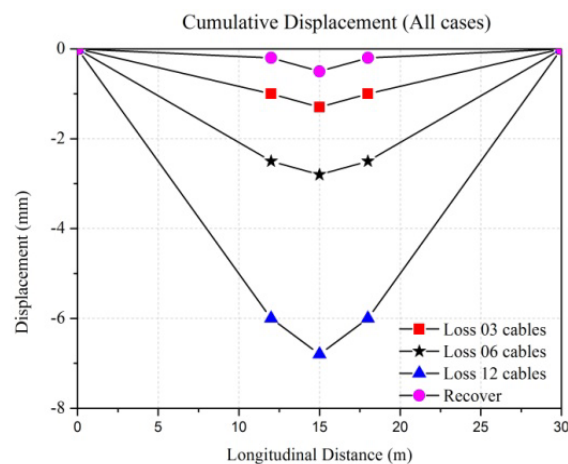


Fig. 27 Displacements under self-weight load considered tendon damage

Table 6 Comparison of natural frequencies during damage test

Nature of modes	Natural Frequencies ( $Hz$ )				
	Intact	03 cable damaged	06 cables damaged	12 cables damaged	Recovered
1 <sup>st</sup> Mode	2.1973	2.1484	2.1484	2.0996	2.1484
2 <sup>nd</sup> Mode	8.2031	8.2031	8.2031	8.2031	8.2031
3 <sup>rd</sup> Mode	16.4063	16.4551	16.4551	16.4063	16.4063

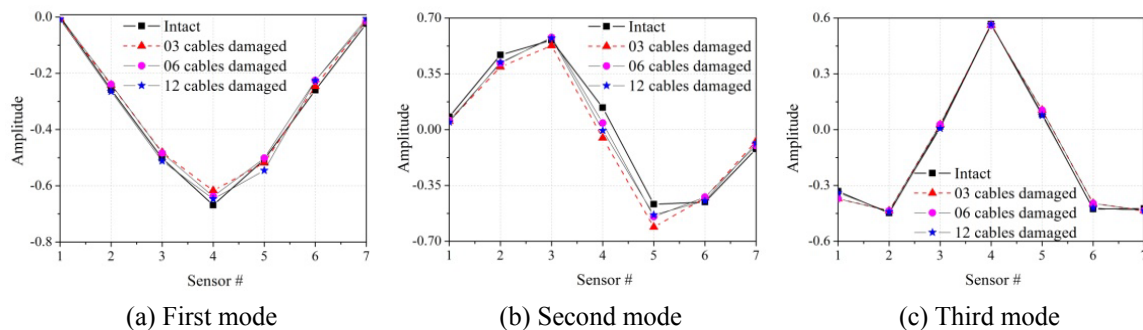


Fig. 28 Comparison of mode shapes

## 6. Conclusions

This paper introduces a new type of composite girder, the concrete filled tubular tied arch girder (CFTA girder). Static and dynamic experiments have been carried out and a FE model has been developed to study the behavior of CFTA girder. Based on the numerical and experimental studies on the behavior of CFTA girder, the following conclusions are drawn:

- A good agreement in CFTA behavior is observed between the numerical and experimental results. The FE model presented in this study can therefore be a reliable tool for identification of tendon damage on the CFTA girder.
- It is observed that all four tendons affect the static behavior of the girder, and the two inside tendons play a more important role in a comparison with the two outside ones.
- The experiments have been carried out for the damage of the cables of outmost tendon. These effects on the CFTA behavior are found to be practically small. It verifies the high safety factor of CFTA girder in case of damage that may take place to outer tendons in use. The changes in strain along the depth and the width of the girder reveal that the most sensitive locations, in the cross section, due to the tendon damage are where anchors are installed to connect arch block and slab.

## Acknowledgements

This research is being funded by Korea Ministry of Land, Transport and Maritime Affairs (MLTM) through Korea Institute of Construction Technology (KICT). The authors express their gratitude for the financial support.

## References

- Chaudhary, S., Pendharkar, U. and Nagpal, A.K. (2009), "Control of creep and shrinkage effects in steel concrete composite bridges with precast decks", *J. Bridge Eng.*, ASCE, **14**(5), 336-345.
- Gardner, N.J. and Jacobson, E.R. (1967), "Structural behavior of concrete filled steel tubes", *ACI J.*, **64**(7), 404-413.
- Ge, H.B. and Usami, T. (1992), "Strength of concrete-filled thin-walled steel box columns: Experiment", *J.*

- Struct. Eng. ASCE*, **118**(11), 3036-3054.
- Ge, H.B. and Usami, T. (1994), "Strength analysis of concrete-filled thin-walled steel box columns", *J. Const. Steel Res.*, **30**(3), 259-281.
- Ge, H.B. and Usami, T. (1996), "Cyclic tests of concrete filled steel box columns", *J. Struct. Eng. ASCE*, **122**(10), 1169-1177.
- Han, L.H. (2000), *Concrete Filled Steel Tubular Structures*, Peking, Science Press.
- Han, L.H., Huang, H. and Zhao, X.L. (2009), "Analytical behaviour of concrete-filled double skin steel tubular (CFDST) beam-columns under cyclic loading", *Thin-Walled Struct.*, **47**(6-7), 668-680.
- Han, L.H., Huang, H., Tao, Z. and Zhao, X.L. (2006), "Concrete-filled double skin steel tubular (CFDST) beam-columns subjected to cyclic bending", *Eng. Struct.*, **28**(12), 1698-1714.
- Knowles, R.B. and Park, R. (1969), "Strength of concrete filled steel tubular columns", *J. Struct. Div. ASCE*, **95**(12), 2565-2587.
- Korea Institute of Construction Technology (KICT) (2010), *A Development of New Type of Girder System Taking Advantage of the Efficiently Composite Structurizing of Structural Construction Materials*, Construction & Transportation R&D Report, Ministry of Construction and Transportation.
- Lee, S.J. (2007), "Capacity and the moment-curvature relationship of high-strength concrete filled steel tube columns under eccentric loads", *Steel Compos. Struct., Int. J.*, **7**(2), 135-160.
- Morcous, G., Hanna, K., Deng, Y. and Maher, T.K. (2010), "Concrete-filled steel tubular tied arch bridge system: Application to Columbus viaduct", *J. Bridge Eng. ASCE*, **17**(1)107-116.
- Sakino, K., Nakahara, H., Morino, S. and Nishiyama, I. (2004), "Behavior of centrally loaded concrete-filled steel-tube short columns", *J. Struct. Eng. ASCE*, **130**(2), 180-188.
- Shams, M. and Saadeghvaziri, M.A. (1999), "Nonlinear response of concrete-filled steel tubular columns under axial loading", *ACI J.*, **96**(6), 1009-1017.
- Susantha, K.A.S., Ge, H.B. and Usami, T. (2001), "Uniaxial stress-strain relationship of concrete confined by various shaped steel tubes", *Eng. Struct.*, **23**(10), 1331-1347.
- Trinh, T.T., Kim, J.H., Park, K.H. and Kong, J.S. (2008), "Dynamic behavior and reliability assessment of a CFTA girder subjected to truck collision", *Int. J. Steel Struct.*, **8**(4), 315-324.
- Xiao, Y., He, W. and Choi, K.K. (2005), "Confined concrete-filled tubular columns", *J. Struct. Eng. ASCE*, **131**(3), 488-497.
- Xiao, Y., He, W. and Choi, K.K. (2010), "Analytical model of circular CFRP confined concrete-filled steel tubular columns under axial compression", *J. Comp. Construct.*, **14**(1), 125-133.
- Yang, Y.F., Han, L.H. and Zhu, L.T. (2009), "Experimental performance of recycled aggregate concrete-filled circular steel tubular columns subjected to cyclic flexural loadings", *Adv. Struct. Eng.*, **12**(2), 183-194.